JOURNAL OF SOLID STATE CHEMISTRY **139,** 326–331 (1998)
ARTICLE NO. SC987851

Synthesis and Characterization of $(C_4H_{12}N_2)_2[Fe_6(HPO_4)_2(PO_4)_6(H_2O)_2]\cdot H_2O$, a New Iron Phosphate Templated by Piperazine

Vítězslav Zima[1] and Kwang-Hwa Lii[2]

Institute of Chemistry, Academia Sinica, Taipei, Taiwan 115, Republic of China

Received November 17, 1997; in revised form April 3, 1998; accepted April 10, 1998

An organically templated iron phosphate, $(C_4H_{12}N_2)_2[Fe_6(HPO_4)_2(PO_4)_6(H_2O)_2]\cdot H_2O$, has been synthesized under hydrothermal conditions and characterized by single-crystal X-ray diffraction, thermogravimetric analysis, and Mössbauer spectroscopy. The compound crystallizes in the triclinic space group $P\bar{1}$ (No. 2) with $a = 9.1768(1)$, $b = 12.7229(1)$, $c = 16.4830(2)$ Å, $\alpha = 68.530(1)$, $\beta = 83.285(1)$, $\gamma = 73.259(1)^\circ$, $V = 1714.90(3)$ Å^3, and $Z = 2$. The structure consists of layers of FeO_6 octahedra and phosphate tetrahedra, which are pillared through FeO_5 trigonal bipyramids and phosphate tetrahedra to form a three-dimensional framework structure. The framework contains infinite channels in which the charge compensating diprotonated piperazinium cations reside. © 1998 Academic Press

INTRODUCTION

Transition metal phosphates with open-framework structures are of interest because of their potential applications as catalysts or ion-exchange materials. Many such compounds were prepared using organic amines as structure-directing agents for the synthesis of microporous materials based on molybdenum and vanadium phosphates (1, 2). Recent progress in hydrothermal synthesis of templated iron phosphates revealed rich structural chemistry of these microporous compounds. Cavellec *et al.* and DeBord *et al.* reported a layered iron phosphate, $[H_3N(CH_2)_2NH_3]_{0.5}Fe(OH)PO_4$ (3, 4), which is isotypic with the corresponding gallophosphate (5). Several fluorinated iron phosphates and a mixed-valence iron phosphate were also reported (6–12). Recently, we have synthesized several iron phosphates containing ethylenediamine (13), 1,3-diaminopropane (14, 15), and 1,4-diazabicyclo[2.2.2]octane (16) as templates. In this paper, we describe the synthesis and the structure of a new iron(III) phosphate, in which piperazine serves as the template. The compound adopts a pillared layer structure.

EXPERIMENTAL

Synthesis and Initial Characterization

All syntheses were carried out in a Teflon-lined acid digestion bomb (23 cm^3) under autogeneous pressure. Hydrothermal treatment of $FeCl_3\cdot 6H_2O$ (2.5 mmol), H_3PO_4 (15 mmol), piperazine (7.5 mmol), and water (9 ml) for 3 days at 180°C yielded a yellow crystalline product of $(C_4H_{12}N_2)_2[Fe_6(HPO_4)_2(PO_4)_6(H_2O)_2]\cdot H_2O$ (further denoted as **1**) together with some white powder and a small amount of black admixture. A yellow crystal was chosen to determine its structure by single-crystal X-ray diffraction. The use of a smaller amount of phosphoric acid (11 mmol) in the reaction under the same conditions led to a homogeneous yellow crystalline product, identical with the yellow crystals obtained from the previous reaction, as was confirmed by powder XRD. The yield was 45% based on iron. Energy-dispersive X-ray fluorescence analysis using a JEOL analytical electron microscope confirmed the presence of Fe and P but no Cl in the yellow crystals. Elemental analysis confirmed the amount of piperazine in the compound. (Found: C, 7.195(7); H, 2.13(6); N, 4.03(7)%. Theoretical: C, 7.23; H, 2.41; N, 4.20%). This product was used for TGA and Mössbauer spectroscopy measurements and elemental analysis.

Thermogravimetric analysis was performed on a Perkin–Elmer TGA 7 thermal analyzer; the sample was heated to 900°C at 10°C min^{-1} in air. The product of heating was identified by powder X-ray diffraction. The ^{57}Fe Mössbauer measurements were made on a constant-acceleration instrument at 300 K. Isomer shift is reported with respect to an iron foil standard.

---

[1] On leave from Joint Laboratory of Solid State Chemistry, University of Pardubice, 533 14 Pardubice, Czech Republic.

[2] To whom correspondence should be addressed.

0022-4596/98 $25.00

Single-Crystal X-Ray Diffraction

A crystal of dimensions 0.1 × 0.1 × 0.2 mm was used for indexing and intensity data collection on a Siemens Smart-CCD diffractometer equipped with a normal focus, 3 kW sealed tube X-ray source. Intensity data were collected in 2082 frames with increasing ω (width of 0.3° per frame). On the basis of statistics of intensity distribution and the successful solution and refinement of the structure, the space group was determined to be $P\bar{1}$. The structure was solved by direct methods: the Fe and P atoms were first located and all the O, C, and N atoms were found in difference Fourier maps. The H atoms were not located. The phosphorus atom of $P(8)O_4$ tetrahedron, its terminal oxygen O(32), and the oxygen of the lattice water molecule O(35w) placed near $P(8)O_4$ are disordered over two positions with occupancy 30 and 70% as depicted in Fig. 1. Disordered atoms with occupancy 30% are referred to as P(8′), O(34), and O(33w). As shown in Fig. 1, water oxygens (O(35w) and O(33w)) are placed opposite to the phosphate oxygens O(32) and O(34), respectively. Least squares refinement was performed by using SHELXTL Version 5 (17), with anisotropic thermal parameters for all atoms. The reliability factors converged to $R1 = 0.0555$ and $wR2 = 0.1406$. Crystallographic data are given in Table 1.

TABLE 1
Crystallographic Data for $(C_4H_{12}N_2)_2[Fe_6(HPO_4)_2(PO_4)_6(H_2O)_2]\cdot H_2O$

Formula	$C_8Fe_6H_{32}N_4O_{35}P_8$
M	1327.2
Crystal system	triclinic
Space group	$P\bar{1}$
a/Å	9.1768(1)
b/Å	12.7229(1)
c/Å	16.4830(2)
α/°	68.530(1)
β/°	83.285(1)
γ/°	73.259(1)
V/Å^3	1714.90(3)
Z	2
D_c/g cm^{-1}	2.570
F(000)	1328
μ/cm^{-1} (Mo$K\alpha$)	29.8
T/°C	23
λ/Å	0.71073
Maximum 2θ/°	57.6
Reflections collected	20201
Unique reflections	8107
Observed unique reflections ($F_0 > 4\sigma(F_0)$)	5317
$T_{\mathrm{min/max}}$	0.602, 0.942
Weight[a]	$a = 0.0547$, $b = 2.24$
Number of parameters	579
R(int)[b]	0.0731
$R1$[c]	0.0555
w$R2$[d]	0.1406
Goodness-of-fit	1.02
$(\Delta\rho)_{\max}$; $(\Delta\rho)_{\min}$/e Å^{-3}	1.01, −0.72

[a] Weight $= 1/[\sigma^2(F_0^2) + (a \times P)^2 + b \times P]$, where $P = (\mathrm{Max}(F_0^2, 0) + 2 \times F_c^2)/3$.

[b] $R(\mathrm{int}) = \sum|F_0^2 - F_0^2(\mathrm{mean})|/\sum[F_0^2]$.

[c] $R1 = \sum||F_0| - |F_c||/\sum|F_0|$

[d] $\mathbf{w}R2 = [\sum[w(F_0^2 - F_c^2)^2]/\sum[w(F_0^2)^2]]^{1/2}$.

RESULTS AND DISCUSSION

Thermogravimetric Analysis and Mössbauer Measurements

The TGA curve of **1** showed total weight loss of 21.5% in three steps over the temperature range 50–750°C (Fig. 2). These three steps correspond to the weight loss of 3 molecules of crystalline water (4.3%, theor.: 4.1%), 3 H_2O from HPO_4^{2-} groups and piperazinium cations (4.3%, theor.: 4.1%), and 2 molecules of piperazine (12.9%, theor.: 13.0%) according to

$$(C_4H_{12}N_2)_2[Fe_6(HPO_4)_2(PO_4)_6(H_2O)_2]\cdot H_2O \rightarrow Fe_4(P_2O_7)_3 + 2FePO_4 + 6H_2O + 2C_4H_{10}N_2 \quad [1]$$

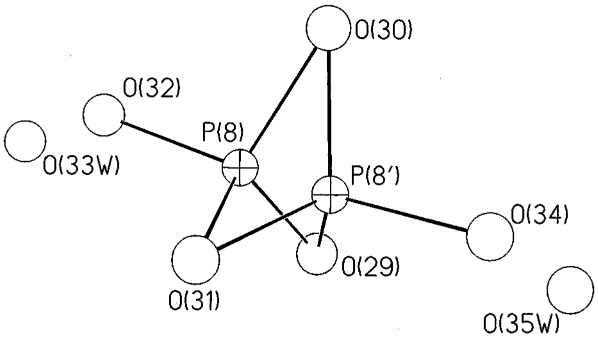

FIG. 1. Disorder in the $P(8)O_4$ tetrahedron.

The existence of $Fe_4(P_2O_7)_3$ and $FePO_4$ in the decomposition products was confirmed by powder XRD (18).

The room-temperature Mössbauer spectrum (Fig. 3) was least-squares fitted by two doublets corresponding to five- and six-coordinated iron atoms with a constraint on the area ratio of 1:2. The obtained parameters are δ (isomer shift) = 0.40 mm s^{-1}, ΔE_Q (quadrupole splitting) = 0.72 mm s^{-1}, and Γ (full width at half height) = 0.30 mm s^{-1} for five-coordinated iron and $\delta = 0.41$ mm s^{-1}, $\Delta E_Q = 0.40$ mm s^{-1}, and $\Gamma = 0.36$ mm s^{-1} for six-coordinated iron. The isomer shifts of both contributions are characteristic of high-spin Fe$^{\mathrm{III}}$. The higher value of quadrupole splitting of five-coordinated iron agrees with its lower symmetry compared to six-coordinated iron. Therefore, the composition of **1** is further defined by TG analysis and Mössbauer spectroscopy.

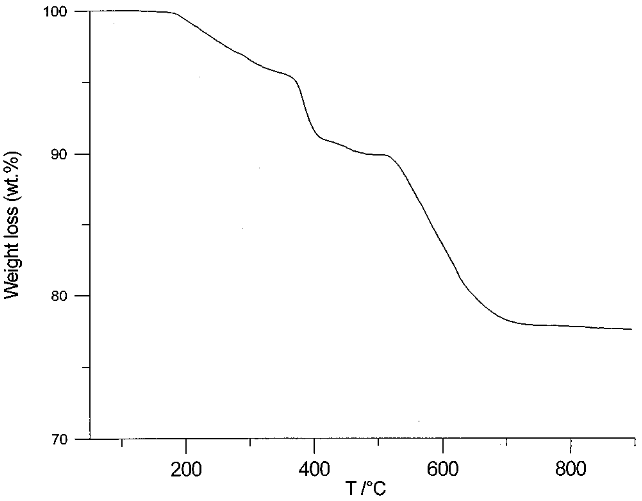

FIG. 2. Thermogravimetric analysis of $(C_4H_{12}N_2)_2[Fe_6(HPO_4)_2(PO_4)_6(H_2O)_2]\cdot H_2O$ in flowing air at 10°C min^{-1}.

Crystal Structure

The atomic coordinates and interatomic distances are given in Tables 2 and 3, respectively. All atoms of compound **1** are at general positions. Fe(3) and Fe(4) are five-coordinate, and all other iron atoms are six-coordinate. Both P(2) and P(8) have terminal P–OH groups as shown by the unsatisfied valence sums for O(8) ($\sum s = 1.10$) and O(32) ($\sum s = 1.13$) and the longer P–O bond lengths [P(2)–O(8) 1.585 and P(8)–O(32) 1.572 Å]. The oxygen atoms O(36w) and O(37w), which are coordinated to iron atoms, are water oxygens as indicated from valence sum calculations ($\sum s = 0.344$ and 0.330 for O(36w) and O(37w), respectively). Atom O(35w) is disordered over two sites and is not bonded to any iron or phosphorus atoms in the structure. Assuming the piperazine molecules to be

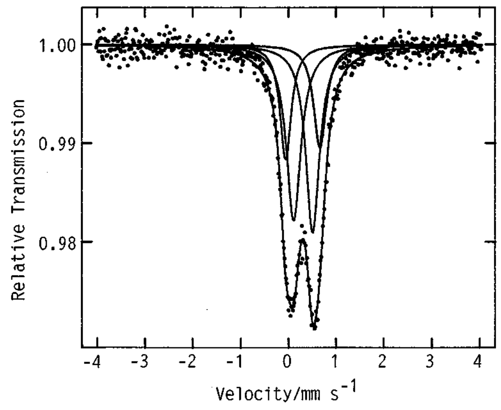

FIG. 3. Mössbauer spectrum of $(C_4H_{12}N_2)_2[Fe_6(HPO_4)_2(PO_4)_6(H_2O)_2]\cdot H_2O$ at 300 K.

TABLE 2
Atomic Coordinates and Thermal Parameters for $(C_4H_{12}N_2)_2[Fe_6(HPO_4)_2(PO_4)_6(H_2O)_2]\cdot H_2O$

Atom	x	y	z	U_{eq} (Å × 100)^a
Fe(1)	0.94514(9)	0.55459(7)	0.12999(5)	1.05(2)
Fe(2)	0.97130(9)	0.06611(7)	0.12269(5)	1.04(2)
Fe(3)	0.31144(9)	0.19092(7)	0.24756(5)	0.95(2)
Fe(4)	0.31093(9)	0.68775(7)	0.25197(5)	0.97(2)
Fe(5)	0.96282(9)	0.44117(7)	0.38236(5)	0.97(2)
Fe(6)	0.96301(9)	0.94138(7)	0.38258(5)	1.04(2)
P(1)	0.0934(2)	0.3087(1)	0.0795(1)	1.08(3)
P(2)	0.6593(2)	0.5223(1)	0.2629(1)	1.21(3)
P(3)	0.1257(2)	– 0.1224(1)	0.0797(1)	1.18(3)
P(4)	0.2275(2)	0.9391(1)	0.2801(1)	0.95(3)
P(5)	0.2194(2)	0.4377(1)	0.27545(9)	0.94(3)
P(6)	0.0527(2)	0.6591(1)	0.4009(1)	1.06(3)
P(7)	0.0471(2)	0.1637(1)	0.4029(1)	1.11(3)
P(8)	0.6708(2)	0.0440(2)	0.2528(1)	1.12(7)
P(8′)	0.6977(6)	0.1083(5)	0.2542(3)	1.1(2)
O(1)	0.0037(5)	0.2176(4)	0.1064(3)	2.1(1)
O(2)	0.2419(5)	0.2617(4)	0.1305(3)	2.1(1)
O(3)	0.9946(5)	0.4189(3)	0.0950(3)	1.77(9)
O(4)	0.8591(5)	0.6621(3)	0.0176(3)	1.75(9)
O(5)	0.7456(4)	0.5293(4)	0.1765(3)	1.71(9)
O(6)	0.5247(4)	0.6287(4)	0.2516(3)	1.9(1)
O(7)	0.7569(4)	0.5083(4)	0.3354(3)	1.80(9)
O(8)	0.5969(5)	0.4108(4)	0.2895(3)	2.0(1)
O(9)	0.1695(4)	– 0.0091(3)	0.0690(2)	1.25(8)
O(10)	0.8743(5)	0.1425(4)	0.0061(2)	1.74(9)
O(11)	0.9677(5)	– 0.1031(4)	0.1231(3)	1.82(9)
O(12)	0.2402(5)	0.7675(3)	0.1355(3)	1.9(1)
O(13)	0.3140(5)	0.0328(3)	0.2495(3)	1.75(9)
O(14)	0.3270(4)	0.8373(3)	0.2552(3)	1.45(9)
O(15)	0.1925(4)	0.9019(3)	0.3794(2)	1.48(9)
O(16)	0.0642(4)	– 0.0145(3)	0.2430(2)	1.37(9)
O(17)	0.0534(4)	0.4661(3)	0.2436(2)	1.24(8)
O(18)	0.3288(4)	0.3425(3)	0.2468(3)	1.54(9)
O(19)	0.2744(4)	0.5485(3)	0.2350(3)	1.51(9)
O(20)	0.1948(4)	0.4000(3)	0.3751(2)	1.34(9)
O(21)	0.2132(5)	0.6571(4)	0.3618(3)	1.84(9)
O(22)	0.9660(4)	0.6070(3)	0.3574(2)	1.39(9)
O(23)	0.9601(5)	0.7851(3)	0.3866(3)	1.9(1)
O(24)	0.9257(5)	0.4129(4)	0.5025(3)	2.0(1)
O(25)	0.1944(5)	0.1723(4)	0.3501(3)	2.1(1)
O(26)	0.9445(4)	0.2861(3)	0.3942(3)	1.75(9)
O(27)	0.9554(5)	0.1053(3)	0.3699(3)	1.67(9)
O(28)	0.9059(5)	0.9067(4)	0.5028(3)	1.9(1)
O(29)	0.7662(4)	0.0872(4)	0.1721(3)	1.9(1)
O(30)	0.5282(4)	0.1396(4)	0.2539(3)	1.88(9)
O(31)	0.7564(4)	0.9982(3)	0.3369(3)	1.61(9)
O(32)^b	0.6150(9)	– 0.0568(6)	0.2440(6)	2.3(2)
O(33w)^b	0.643(3)	– 0.128(3)	0.247(2)	6.6(8)
O(34)^b	0.734(2)	0.211(2)	0.264(1)	3.9(6)
O(35w)^b	0.784(1)	0.262(1)	0.2390(8)	7.0(3)
O(36w)	0.8874(5)	0.6965(3)	0.1795(3)	1.79(9)
O(37w)	0.1496(4)	0.6097(3)	0.0771(3)	1.58(9)
N(1)	0.6667(6)	0.7588(5)	0.4705(3)	2.3(1)
N(2)	0.3565(6)	0.7479(5)	0.5197(3)	2.2(1)
N(3)	0.6377(6)	0.4906(5)	0.0406(4)	2.6(1)
N(4)	0.3774(7)	0.0399(5)	– 0.0622(4)	3.3(1)

TABLE 2—*Continued*

Atom	x	y	z	U_{eq} (Å × 100)[a]
C(1)	0.5503(7)	0.8609(6)	0.4860(4)	2.6(2)
C(2)	0.4308(7)	0.8173(6)	0.5515(4)	2.5(2)
C(3)	0.4726(8)	0.6474(6)	0.5018(4)	2.6(2)
C(4)	0.5913(8)	0.6937(6)	0.4358(5)	3.0(2)
C(5)	0.5237(8)	0.6077(6)	0.0031(5)	3.0(2)
C(6)	0.5652(8)	0.3919(6)	0.0707(5)	3.1(2)
C(7)	0.4898(9)	− 0.0795(7)	− 0.0419(5)	3.6(2)
C(8)	0.4503(8)	0.1244(6)	− 0.0520(5)	3.3(2)

[a] U_{eq} is defined as one-third of the trace of the orthogonalized $\mathbf{U}_{ij}$ tensor.
[b] Occupancy factors for O(32), O(33), O(34), and O(35) are 0.711(7), 0.289(7), 0.711(7), and 0.289(7), respectively.

dications, O(35w) can be ascribed to a neutral water molecule occluded in the cavity surrounded by P(8)O_4 tetrahedron and Fe(2)O_6 and Fe(6)O_6 octahedra. This water oxygen forms H-bonds to the hydroxo oxygen O(8) and to O(1), O(27), and O(29) as inferred from the O–O distances of 2.5 to 2.9 Å.

The structure of **1** is formed of two similar structural units (Fig. 4). In both of them, two octahedral Fe centers share a common vertex which is a μ_3-oxygen atom. The third coordination of this oxygen is completed by the phosphorus of a phosphate tetrahedron, which shares an edge with one of the FeO_6 octahedra. This octahedron is strongly distorted due to edge sharing. Other corners of this PO_4 tetrahedron are linked to Fe(3)O_5 and Fe(4)O_5 trigonal bipyramids. In addition, a HPO_4 group bridges over FeO_6 octahedra in the dimer. The two structural units are connected to other units via phosphate groups in different ways. The Fe(1)O_6 octahedron shares two corners with two P(1)O_4 groups and the remaining coordination positions are completed by two water oxygens. The corresponding octahedron, Fe(2)O_6, in the second structural unit has no terminal oxygen atom and is connected to other structural units by corner shared P(1)O_4 and P(3)O_4 and edge shared P(3)O_4 tetrahedra. As shown in Figs. 5 and 6, the structural units are connected to form macroanionic sheets in the (100) plane which are linked through phosphate tetrahedra and FeO_5 trigonal bipyramids to form a three-dimensional framework. The framework contains channels with eight-sided windows parallel to the [010] direction, in which the charge compensating diprotonated piperazinium cations reside. An alternative way of describing the structure is that it consists of layers of FeO_6 octahedra and phosphate tetrahedra, which are pillared through FeO_5 and phosphate groups. Within the infinite channels are 8-membered rings formed by the edges of two octahedra, two trigonal bipyramids, and four tetrahedra. The piperazinium cations are anchored to the framework by forming H-bonds with the oxygens of the framework with N ··· O distances in the range 2.70–3.03 Å.

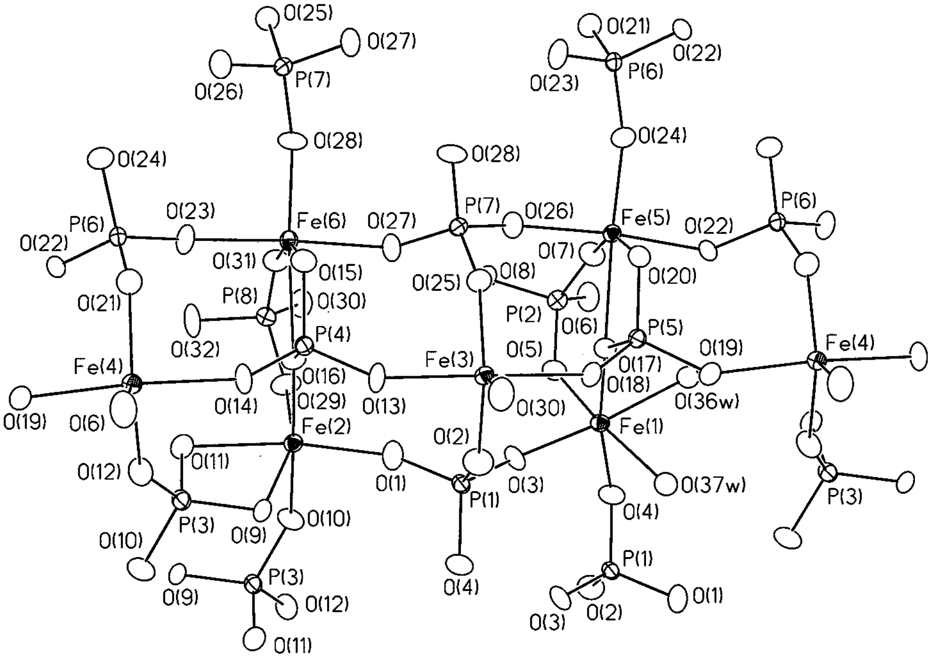

FIG. 4. Structural units of $(C_4H_{12}N_2)_2[Fe_6(HPO_4)_2(PO_4)_6(H_2O)_2] \cdot H_2O$ viewed approximately along the [100] direction. Thermal ellipsoids are shown at 60% probability. O(36w) and O(37w) are water oxygen atoms.

TABLE 3
Interatomic Distances (Å) for $(C_4H_{12}N_2)_2[Fe_6(HPO_4)_2(PO_4)_6(H_2O)_2] \cdot H_2O$

Fe(1)–O(3)	1.933(4)	Fe(1)–O(4)	1.947(4)
Fe(1)–O(5)	1.968(4)	Fe(1)–O(17)	2.002(4)
Fe(1)–O(36w)	2.153(4)	Fe(1)–O(37w)	2.168(4)
Fe(2)–O(1)	1.952(4)	Fe(2)–O(9)	2.061(4)
Fe(2)–O(10)	1.992(4)	Fe(2)–O(11)	2.160(4)
Fe(2)–O(16)	2.029(4)	Fe(2)–O(29)	1.946(4)
Fe(3)–O(2)	1.904(4)	Fe(3)–O(13)	1.994(4)
Fe(3)–O(18)	1.976(4)	Fe(3)–O(25)	1.870(4)
Fe(3)–O(30)	1.909(4)	Fe(4)–O(6)	1.888(4)
Fe(4)–O(12)	1.902(4)	Fe(4)–O(14)	1.971(4)
Fe(4)–O(19)	2.014(4)	Fe(4)–O(21)	1.881(4)
Fe(5)–O(7)	1.957(4)	Fe(5)–O(17)	2.280(4)
Fe(5)–O(20)	2.041(4)	Fe(5)–O(22)	2.005(4)
Fe(5)–O(24)	1.886(4)	Fe(5)–O(26)	1.965(4)
Fe(6)–O(15)	2.018(4)	Fe(6)–O(16)	2.307(4)
Fe(6)–O(23)	1.973(4)	Fe(6)–O(27)	2.000(4)
Fe(6)–O(28)	1.910(4)	Fe(6)–O(31)	1.957(4)
P(1)–O(1)	1.518(4)	P(1)–O(2)	1.534(4)
P(1)–O(3)	1.526(4)	P(1)–O(4)	1.545(4)
P(2)–O(5)	1.533(4)	P(2)–O(6)	1.516(4)
P(2)–O(7)	1.505(4)	P(2)–O(8)	1.577(4)
P(3)–O(9)	1.550(4)	P(3)–O(10)	1.526(4)
P(3)–O(11)	1.535(4)	P(3)–O(12)	1.533(4)
P(4)–O(13)	1.522(4)	P(4)–O(14)	1.516(4)
P(4)–O(15)	1.550(4)	P(4)–O(16)	1.552(4)
P(5)–O(17)	1.568(4)	P(5)–O(18)	1.518(4)
P(5)–O(19)	1.526(4)	P(5)–O(20)	1.542(4)
P(6)–O(21)	1.534(4)	P(6)–O(22)	1.540(4)
P(6)–O(23)	1.527(4)	P(6)–O(24)	1.523(4)
P(7)–O(25)	1.528(4)	P(7)–O(26)	1.535(4)
P(7)–O(27)	1.522(4)	P(7)–O(28)	1.523(4)
P(8)–O(29)	1.519(4)	P(8)–O(30)	1.512(4)
P(8)–O(31)	1.510(4)	P(8)–O(32)	1.568(8)
P(8′)–O(29)	1.507(6)	P(8′)–O(30)	1.491(6)
P(8′)–O(31)	1.566(7)	P(8′)–O(34)	1.50(2)
N(1)–C(1)	1.508(8)	N(1)–C(4)	1.504(8)
N(2)–C(2)	1.513(8)	N(2)–C(3)	1.509(8)
N(3)–C(5)	1.508(9)	N(3)–C(6)	1.488(8)
N(4)–C(7)	1.512(9)	N(4)–C(8)	1.485(9)
C(1)–C(2)	1.521(9)	C(3)–C(4)	1.529(9)
C(5)–C(6)	1.539(9)	C(7)–C(8)	1.55(1)

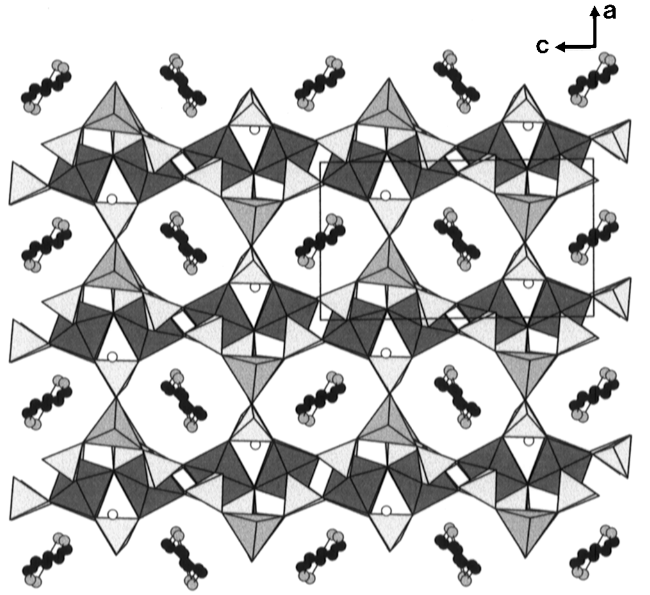

FIG. 5. Polyhedral representation of the $(C_4H_{12}N_2)_2[Fe_6(HPO_4)_2(PO_4)_6(H_2O)_2] \cdot H_2O$ structure viewed along the [010] direction. Polyhedra with darker and lighter shade are FeO_6 octahedra and FeO_5 trigonal bipyramids, respectively; tetrahedra are PO_4 groups; (solid circles), C; (stippled circles), N; (open circles), lattice water oxygen atoms.

In conclusion, the hydrothermal synthesis described in this work produces another example of an organic molecule templated open-framework structure of iron phosphate. The reaction mixture for the synthesis of the title compound is slightly acidic in contrast to other organically templated iron phosphates described previously (13–16). The formation of iron phosphates is much affected by the pH conditions, which can be adjusted by the addition of an organic base. Acidity of the starting mixture also governs the size of the crystals and homogeneity of the product. Crystals are generally larger at lower pH values, but the amount of by-products is higher. Homogeneous product with fine crystals is obtained at higher pH values, with acid/template molar ratio of about 1.5. Piperazine appears to be a versatile structure-directing agent. Several new open-framework iron phosphates with encapsulated piperazinium cations have been prepared and will be presented in future publications.

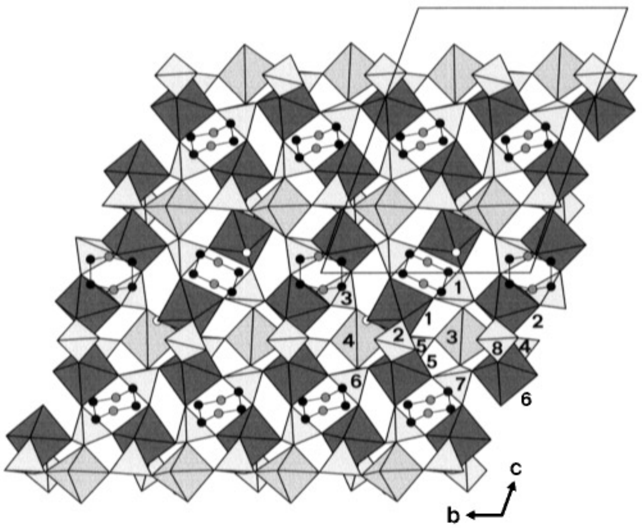

FIG. 6. A layer of the $(C_4H_{12}N_2)_2[Fe_6(HPO_4)_2(PO_4)_6(H_2O)_2] \cdot H_2O$ structure viewed along [100]. Numbers refer to the labels of iron and phosphorus atoms.

ACKNOWLEDGMENTS

We thank the Institute of Chemistry, Academia Sinica, and the National Science Council (NSC87-2113-M-001-019) for support, Professor S.-L. Wang and Ms. F.-L. Liao at the National Tsing Hua University for X-ray intensity data collection, and Professor T.-Y. Dong at the National Sun Yat-Sen University for Mössbauer spectroscopy measurements.

REFERENCES

1. R. C. Haushalter and L. A. Mundi, *Chem. Mater.* **4,** 31 (1992) and references cited therein.
2. M. I. Khan, L. M. Meyer, R. C. Haushalter, A. L. Schweitzer, J. Zubieta, and J. L. Dye, *Chem. Mater.* **8,** 43 (1996) and references cited therein.
3. M. Cavellec, D. Riou, and G. Ferey, *Acta Crystallogr. Sect. C* **51,** 2242 (1995).
4. J. R. D. DeBord, W. M. Reiff, R. C. Haushalter, and J. Zubieta, *J. Solid State Chem.* **125,** 186 (1996).
5. R. H. Jones, J. M. Thomas, H. Qisheng, M. B. Hursthouse, and J. Chen, *J. Chem. Soc. Chem. Commun.* 150 (1991).
6. M. Cavellec, D. Riou, and G. Ferey, *J. Solid State Chem.* **112,** 441 (1994).
7. M. Cavellec, D. Riou, and G. Ferey, *Eur. J. Solid State Inorg. Chem.* **32,** 271 (1995).
8. M. Cavellec, D. Riou, C. Ninclaus, J. M. Greneche, and G. Ferey, *Zeolites* **17,** 250 (1996).
9. M. Cavellec, D. Riou, J. M. Greneche, and G. Ferey, *J. Magn. Magn. Mat.* **163,** 173 (1996).
10. M. Cavellec, D. Riou, J. M. Greneche, and G. Ferey, *Microporous Mater.* **8,** 103 (1997).
11. M. Cavellec, D. Riou, J. M. Greneche, and G. Ferey, *Inorg. Chem.* **36,** 2187 (1997).
12. J. R. D. DeBord, W. M. Reiff, C. J. Warren, R. C. Haushalter, and J. Zubieta, *Chem. Mater.* **9,** 1994 (1997).
13. C. Y. Huang, S. L. Wang, and K. H. Lii, *J. Porous Mater.* **5,** 147 (1998).
14. K. H. Lii and Y. F. Huang, *J. Chem. Soc. Chem. Commun.* 839 (1997).
15. K. H. Lii and Y. F. Huang, *J. Chem. Soc. Chem. Commun.* 1311 (1997).
16. K. H. Lii and Y. F. Huang, *J. Chem. Soc. Dalton Trans.* 2221 (1997).
17. G. M. Sheldrick, “SHELXTL PC, Version 5,” Siemens Analytical X-Ray Instruments Inc., Madison WI, 1995.
18. $Fe_4(P_2O_7)_3$, file number 36-318; $FePO_4$, 29-715; Joint Committee on Powder Diffraction Standards, International Centre of Diffraction Data, Swarthmore, PA.